Gramicidin Channels

Olaf S. Andersen, Roger E. Koeppe, II, and Benoît Roux

***Abstract*—Gramicidin channels are mini-proteins composed of two tryptophan-rich subunits. The conducting channels are formed by the transbilayer dimerization of nonconducting subunits, which are tied to the bilayer/solution interface through hydrogen bonds between the indole NH groups and the phospholipid backbone and water. The channel structure is known at atomic resolution and the channel's permeability characteristics are particularly well defined: gramicidin channels are selective for monovalent cations, with no measurable permeability to anions or polyvalent cations; ions and water move through a pore whose wall is formed by the peptide backbone; and the single-channel conductance and cation selectivity vary when the amino acid sequence is varied, even though the permeating ions make no contact with the amino acid side chains. Given the amount of experimental information that is available—for both the wild-type channels and for channels formed by amino acid-substituted gramicidin analogues—gramicidin channels provide important insights into the microphysics of ion permeation through bilayer-spanning channels. For the same reason, gramicidin channels constitute the system of choice for evaluating computational strategies for obtaining mechanistic insights into ion permeation through the complex channels formed by integral membrane proteins.**

***Index Terms*—Kinetics of ion permeation, molecular dynamics, single-channel electrophysiology, structure–function studies.**

I. Introduction

THE LINEAR gramicidins are a family of antibiotics that exert their antibacterial activity by increasing the cation permeability of the target bacterial plasma membrane [1], due to the formation of bilayer-spanning channels [2]. Compared to channels formed by other antibiotics, the gramicidin channels are exceptionally well behaved, which, together with their cation selectivity and the existence of an atomic-level model for the channel structure, the single-stranded (SS) β-helical dimer [3], [4], makes gramicidin channels important tools for understanding the microphysics of ion permeation through bilayer-spanning channels.

Gramicidin channels are arguably the best understood ion channels. Atomic (or near-atomic) resolution structures have been reported for an increasing number of ion channels [5]–[13], but gramicidin channels continue to provide a unique combination of advantages that sets them apart from other channels: the structure of the bilayer-spanning channel is known; there is a wealth of information about its ion permeability; the ion permeability can be modulated by defined chemical modifications whose influence on structure can be determined experimentally; and the wild-type and amino-substituted analogue channels are large enough to be nontrivial and yet small enough to be amenable to detailed computational studies.

We review first the channel structure and dynamics and show that even though the linear gramicidins are conformationally polymorphic in organic solvents, the structure in lipid bilayers, or bilayer-like environments, is remarkably well defined. We then discuss the channels' permeability properties; finally we show how molecular dynamics (MD) simulations have reached the point where there is semiquantitative agreement between observed and predicted ion permeabilities.

Manuscript received November 4, 2004; revised November 15, 2004. This work was supported in part by the National Institutes of Health (NIH) under Grants GM21342 (awarded to O. S. Andersen), RR15569 (awarded to R. E. Koeppe), and GM62342 (awarded to B. Roux).

O. S. Andersen and B. Roux are with the Weill Medical College of Cornell University, New York, NY 10021 USA (e-mail: sparre@med.cornell.edu; benoit.roux@med.cornell.edu).

R. E. Koeppe, II, is with the University of Arkansas, Fayetteville, AR 72701 USA (e-mail: rk2@uark.edu).

Digital Object Identifier 10.1109/TNB.2004.842470

II. Structure

The linear gramicidins, exemplified by [Val^1]gramicidin A (gA), have an alternating L-D-amino acid sequence [14]

Formyl−L−Val−−−Gly−L−Ala−D−Leu−L−Ala−
−D−Val−L−Val−D−Val−L−Trp−D−Leu−L−Trp−
−D−Leu−L−Trp−D−Leu−L−Trp−ethanolamine

which allows the molecule to fold as a helix with the side chains projecting from the exterior surface of a cylindrical tube formed by the peptide backbone [3], [15]. Many such folding patterns are possible, and gA is conformationally polymorphic [16]. Common to the observed conformers is that the helices are stabilized by hydrogen bonds between the backbone CO and NH functions. At least seven such structures have been described in organic solvents, where gA forms a variety of double-stranded (DS) intertwined dimers [17]–[21].

A. One Conducting Channel Conformation

In lipid bilayers or bilayer-like environments, however, the channel's electrophysiological "fingerprint" (single-channel current traces, Fig. 1, and current transition amplitude and lifetime distributions, Fig. 2) show that there is only a single conducting channel structure. The luminal diameter of the pore that is formed by peptide backbone is ~ 4 Å, as determined from the channel's permeability to alkali metal cations, H^+, and water [22]–[24]. These constraints allowed for a refinement of the β-helical structure [4], which taken together with results from single-channel [25], [26] and nuclear magnetic resonance (NMR) studies [27], [28] established gA channels to be antiparallel SS $\beta^{6.3}$-helical dimers [29].

B. Atomic Resolution Structure

The atomic resolution structure was determined by solution and solid-state NMR [30]–[32]; the channel is an antiparallel formyl-NH-terminal-to-formyl-NH-terminal dimer formed by

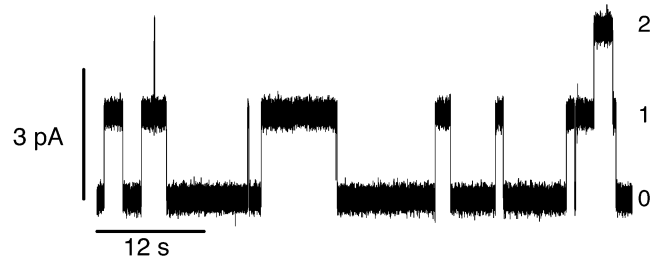

Fig. 1. Single-channel current trace obtained with the gA analogue [D-Ala^2, Ser^3]gA in a diphytanoylphosphatidylcholine (DPhPC)/*n*-decane bilayer. The numbers to the right of the trace denote the number of conducting channels at the different current levels. The analogue forms a single type of ion-permeable channels with well-defined current transitions. The conducting state is "stable," meaning that the current noise of the conducting state is indistinguishable from that of the baseline: the standard deviation (SD) of level 0 is 0.136 pA; for level 1, 0.136 pA; for level 2, 0.133 pA. Electrolyte solution: 1.0 M NaCl, pH 7; applied potential 200 mV; current signal filtered at 500 Hz.

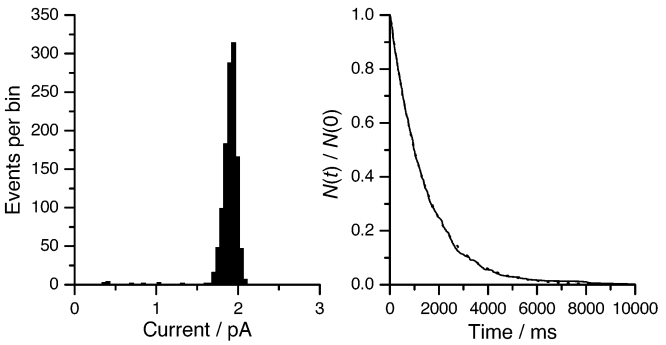

Fig. 2. Characterization of [D-Ala^2, Ser^3]gA channel function. Left: current transition amplitude histogram. There is a single predominant peak at 1.9 pA, which comprises 1175 of the 1202 transitions. Right: lifetime distribution, as normalized survivor plot. The stippled curve is a fit of $N(t)/N(0) = \exp\{-t/\tau\}$ to the results, where $N(t)$ is the number of channels with lifetime longer than time t, and τ the average lifetime (1410 ms). Experimental conditions as in Fig. 1.

right-handed (RH) SS $\beta^{6.3}$-helical subunits, which are joined by six intermolecular hydrogen bonds (Fig. 3). (Minor differences between the reported Protein Data Base (PDB) structures based on solid-state and solution NMR (PDB : 1MAG and PDB : 1JNO, respectively), can be reconciled through MD analysis of the structures [33].) Apart from the helix being right-handed, rather than left-handed, the structure is remarkably similar to the one proposed by Urry more than 30 years ago [3], [4].

Even though the gA channel's molecular weight is only ~4 kDa, the results in Figs. 1–3 show that the channels have the structural and functional definition expected for more complex membrane proteins—features that continue to put gA channels in a class of their own. In fact, the current transitions in Fig. 3 show much less "excess noise" than the current transitions observed in channels formed by integral membrane proteins, e.g., KcsA channels [36] and Ca^{2+}-activated potassium channels [37], such that one with some certainty can relate the measured function to a specific, albeit dynamic [33], structure. Gramicidin channels should be considered to be mini-proteins.

C. Importance of the Tryptophans

The four Trp residues in each subunit are important determinants of the channel fold because the indole NH groups can

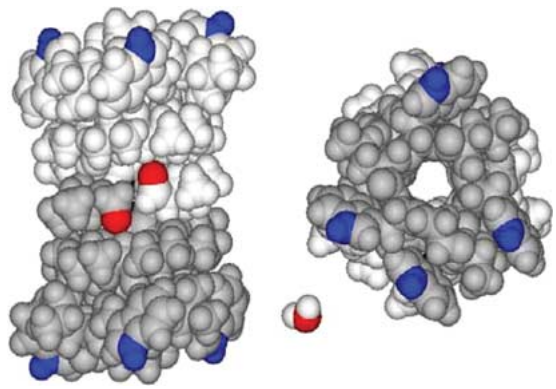

Fig. 3. Side and end views of the bilayer-spanning gA channel. The energy-minimized structure represents a composite consistent with the several NMR-determined structures [31], [32], [34], [35]. The two subunits are shaded differently. The formyl oxygens are red, and the indole NHs are blue. The four Trp indole rings cluster near each membrane/solution interface. (For comparison, a water molecule is shown).

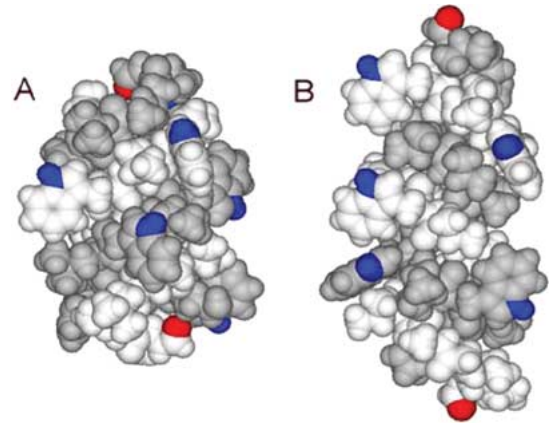

Fig. 4. Side views of two DS gA conformers crystallized from organic solvents. (A) Structure crystallized from CsCl/methanol or from acetic acid [20]. (B) Structure crystallized from ethanol [19]. As in Fig. 3, the two subunits are shaded differently: the formyl oxygens are red, and the indole NHs are blue. In contrast to Fig. 3, in the DS structures the Trp indole rings do not cluster near the ends, but are distributed rather evenly along the dimer.

form hydrogen bonds to polar residues at the bilayer/solution interface [38], which would favor SS over DS conformers [39]. Indeed, the conformational plethora in organic solutes shows that the intrinsic gA folding preference is to form intertwined DS structures in which the Trp residues are distributed along the dimer (Fig. 4). When the DS conformers encounter lipid bilayers membranes, they unfold/refold into the Trp-anchored SS structure in Fig. 3 [40].

This preference to fold into SS channels in lipid bilayers (or bilayer-like environments) arises from the energetic penalty associated with burying the Trp residues in the bilayer hydrophobic core; indeed, gA analogues with multiple Trp→Phe substitutions form a variety of DS structures in lipid bilayers [41], [42]. The organization of Trp residues in integral membrane proteins mirrors that observed in gA channels [43], presumably due to the same energetic principles that were deduced for gA channels.

The bilayer-spanning SS dimers are perpendicular to the bilayer [44]–[46]; in solid-state NMR, the average wobble is zero and the principal order parameter is 0.93 [47]. The Trp residues

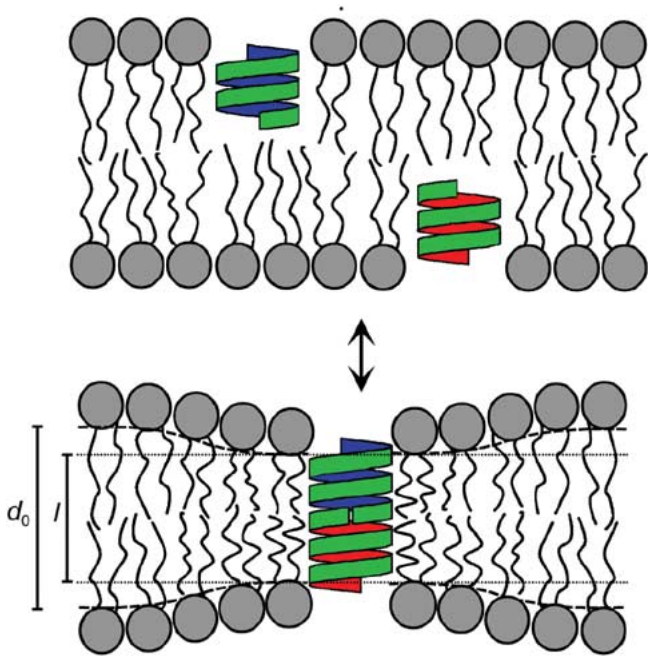

Fig. 5. gA channels formed by the transbilayer dimerization of two RH, SS $\beta^{6,3}$-helical subunits. When the channel's hydrophobic length (l) differs from the average thickness of the unperturbed bilayer hydrophobic core (d_0), channel formation will be associated with a bilayer deformation [62], due to the compression and bending of the two bilayer leaflets.

wobble only slightly more than the backbone [48], although there may be transitions between different "conventional" rotamer positions [33]; the Val side chains likewise occupy canonical rotamer positions, with two rigid and two hopping [49]. Two rotamers have been reported for Trp^9 in lipid bilayers [31], [50]; one is similar to the dominant rotamer in SDS micelles [32], [34]. As shown by MD analysis of the structures [33], both Trp^9 rotamers are compatible with a variety of solid-state NMR measurements; but a weighted average of the two conformers provides the best fit to the results. Such a weighted average, with rapid interconversion between the rotamers, can also account also for fluorescence results that suggest Trp^9 and Trp^{15} quench each other [51], [52].

D. Importance of the Bilayer-Channel Hydrophobic Match

The shift in conformational preference between the polymorphic behavior in organic solvents and the unique structure in lipid bilayers is but one example of environment-dependent folding. The preference to fold into SS dimers depends on the hydrophobic "match" between bilayer thickness and channel length [53]. Following Mouritsen and Bloom [54], exposing hydrophobic residues to water incurs an energetic cost [55], [56]. A hydrophobic mismatch between the channel's hydrophobic length (l) and the average thickness of the unperturbed bilayer hydrophobic core (d_0) will, therefore, cause the bilayer to deform (Fig. 5) [57], [58]. (Because lipid bilayers are in the liquid-crystalline state, the bilayer/solution interface undergoes thermal fluctuations [59], which involve the local movement of individual phospholipid molecules, as well as more global bilayer undulations and peristaltic motions [59], [60]. The bilayer/solution interface, thus, is "fuzzy"; but the *average* bilayer thickness is a well-defined parameter).

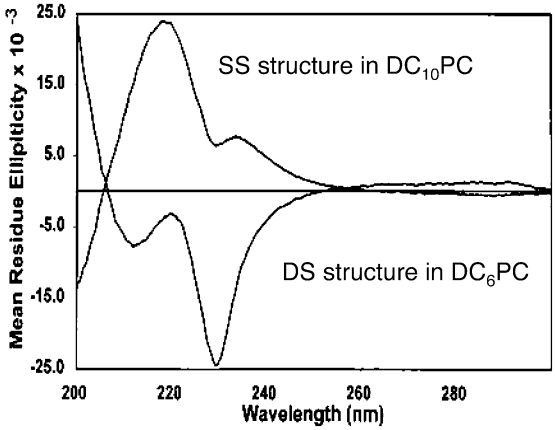

Fig. 6. CD spectroscopic "signatures" for the channel conformation of gA in Di-C_{10}-PC bilayers, and for the nonchannel conformation in Di-C_6-PC micelles. Adapted from Greathouse *et al.* [53].

The bilayer thickness-dependent folding arises because the deformation has an associated energetic cost [57], which can be expressed as [61]

$$\Delta G^0_{\rm def} = H_B \cdot (d_0 - l)^2 \tag{1}$$

where H_B is a phenomenological spring constant whose magnitude is determined by the bilayer compression and bending moduli, as well as d_0 and the channel radius [61]. The thickness-dependent conformational preference thus arises because $\Delta G^0_{\rm def}$ contributes to the overall free energy change (ΔG^0) associated with the gA monomer $\leftrightarrow$ dimer equilibrium.

Assuming that ΔG^0 can be expressed as the sum of intrinsic contributions, due to the formation of the hydrogen bond-stabilized dimer $(\Delta G^0_{\rm prot})$, and extrinsic contributions due to the bilayer deformation, $\Delta G^0_{\rm def}$, the equilibrium constant for the monomer $\leftrightarrow$ dimer equilibrium becomes

$$K = \frac{[D]}{[M]^2} = \exp\left\{\frac{-\Delta G^0}{k_B T}\right\} = \exp\left\{\frac{-\left(\Delta G^0_{\rm prot} + \Delta G^0_{\rm def}\right)}{k_B T}\right\} \tag{2}$$

where [M] and [D] denote the mole-fractions of gA monomers and dimers in the bilayer. Because $\Delta G^0_{\rm def}$ varies as a function of $(d_0 - l)^2$, the energetic penalty for inserting a bilayer-spanning SS dimer eventually becomes so large that other conformers, e.g., the DS structures, become favored [53], [55], [56].

Given this context, the RH, SS $\beta^{6,3}$-helical dimer is remarkably robust: it is preserved in bilayers with acyl chain lengths varying between C_{10} and $C_{20:1}$ [53], [55], [56], [63] and even in sodium dodecyl sulfate (SDS) micelles [32]–[34]. Fig. 6 shows the characteristic circular dichroism (CD) signatures for gA incorporated into di-C_{10}-phosphatidylcholine $(DC_{10}PC)$, where it is in the RH, SS $\beta^{6,3}$-helical conformation, and into DC_6PC, where it is in a DS conformation.

E. Structural Equivalence of gA Mutants

Not only is the channel structure remarkably stable and well-defined, the basic fold and peptide backbone organization do

not vary when the amino acid sequence is varied (as long as the alternating L–D sequence, and the aromatic–aliphatic organization in the carboxy-ethanolamide half of the sequence, are maintained). To test whether a mutant gramicidin, e.g., [D–Ala^2, Ser^3]gA, forms channels that are structurally equivalent to the native gA channels, we exploit the fact that gA channels are symmetric, antiparallel dimers formed by the transmembrane association of nonconducting $\beta^{6.3}$-helical subunits residing in each leaflet of the bilayer (Fig. 5). Then, if two different gA analogues (A and B) form homodimeric (AA and BB) channels that have the same structure, meaning the same peptide backbone fold, one should be able to observe the formation of heterodimeric (AB and BA) channels [26], [64], [65]. Moreover, if the AA and BB channels differ in their current transition amplitudes, the heterodimeric (AB or BA) channels should have current transitions in between those of the AA and BB channels. Further, if the potential of mean force (PMF) for ion movement through the heterodimeric channels is asymmetric, the current in the A $\rightarrow$ B direction should differ from the current in the B $\rightarrow$ A direction.

Formally, hybrid channel formation can be described as an equilibrium between the symmetric homodimers and asymmetric heterodimers

$$\mathsf{AA} + \mathsf{BB} \rightleftarrows \mathsf{AB} + \mathsf{BA}.$$

If AA and BB are structurally equivalent, the distribution between AA, BB, AB, and BA will be given by [65]

$$f_{\mathsf{AB}} \cdot f_{\mathsf{BA}} = f_{\mathsf{AA}} \cdot f_{\mathsf{BB}}. \tag{3}$$

In case AB and BA are indistinguishable, (3) reduces to the binomial distribution [64]

$$f_{\mathsf{AB}} + f_{\mathsf{BA}} = 2 \cdot \sqrt{f_{\mathsf{AA}} \cdot f_{\mathsf{BB}}}. \tag{4}$$

The physical interpretation of the relative heterodimer appearance rate being close to the predictions of (3) [and (4)] is that there is no subunit-specific barrier to the formation of heterodimers, as compared to homodimers [64], [65].

The relative heterodimer appearance rates in Fig. 7 conform to the predictions of (3): ($f_{\mathsf{AB}} \cdot f_{\mathsf{BA}} / f_{\mathsf{AA}} \cdot f_{\mathsf{BB}} = 0.96$). We conclude that Ala→Ser (and Gly→D-Ala) substitutions are well tolerated in the $\beta^{6.3}$-helical fold. Similar results have been obtained with many other gA mutants [64], [66]–[69], and the approach has been verified by NMR [70], [71]. (The test for structural equivalence can be pursued further by examining the single-channel lifetime distributions for the channels [64], [65]).

III. Channel Function

gA channels are seemingly ideally selective for monovalent cations [23], meaning that single-channel measurements provide direct information about the net cation flux through the channel. The pore radius restricts ions and water to move in single file through the pore [72], [73]; but the rate of ion movement through the channels is large enough to allow single-channel measurements to be done over a wide range of permeant ion concentrations and potentials [22], [74], [75]. Moreover, the current through gA channels usually has little

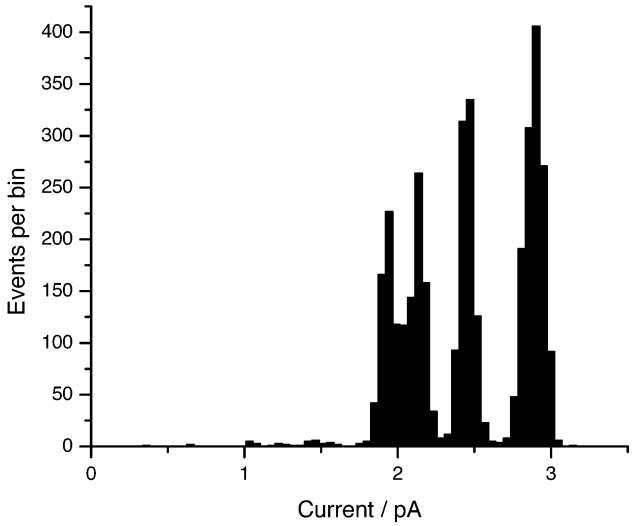

Fig. 7. Structural equivalence of gA and [D-Ala^2,Ser^3]gA channels. Current transition amplitude histogram obtained when [D-Ala^2,Ser^3]gA and gA both are added to both sides of a lipid bilayer. The four peaks represent (from left to right): [D-Ala^2,Ser^3]gA homodimers; [D-Ala^2, Ser^3]gA/gA heterodimers; gA/[D-Ala^2,Ser^3]gA heterodimers; and gA homodimers. The identities of the heterodimers were determined by adding [D-Ala^2,Ser^3]gA to only side of a bilayer and gA to only the other side (results not shown).

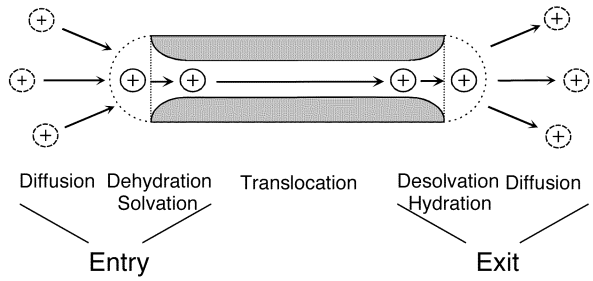

Scheme I

"excess" noise (cf. Fig. 1, where the SD of the current noise does not vary when a channel forms), in contrast to the situation in channels formed by integral membrane proteins. Moreover, the $\beta^{6.3}$-helical channel conformation does not vary as a function of the permeant ion type or concentration [76], [77].

A. Kinetics of Channel-Catalyzed Ion Movement

Generally, movement through a channel can be decomposed into several steps (Scheme I): ion entry—diffusion to channel entrance and association with the pore (dehydration and resolvation by polar groups in the pore wall); translocation through the channel interior, and ion exit—dissociation from the pore (desolvation/rehydration) and diffusion out into the other bulk solution.

This decomposition of the ion transfer into a series of discrete steps is an approximation because each step represents an electrodiffusive barrier crossing, but it summarizes the essential features, which also can be deduced by inspection of the PMF (see Fig. 10, Section IV). Scheme I, thus, serves as a convenient reference for the analysis of experiments on channels formed by gA and amino acid-substituted analogues.

NMR [78] and X-ray scattering [79] results show two major cation binding sites in the channel, one at either end, with no

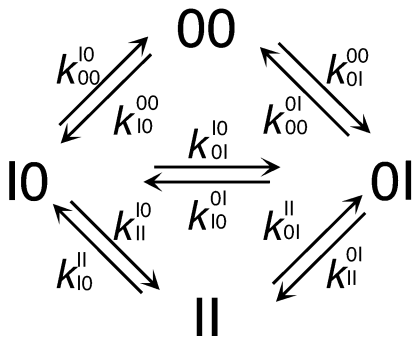

Scheme II

significant ion occupancy outside these two sites. The two sites can be occupied simultaneously [80], such that a minimal kinetic model for ion permeation becomes the three-barrier-two-site-two-ion (3B2S2I) model depicted in Scheme II: in which "0" and "I" denote whether a site (in the left or right half of the channel) is empty or occupied. The rate constants k^{ii}_{ff} (where the super- and subscripts denote the initial and final states, respectively) are functions of the applied voltage

$$k^{ii}_{ff} = \kappa^{ii}_{ff} \cdot f^{ii}_{ff}(V) \tag{5}$$

where κ^{ii}_{ff} denotes the 0 mV value for a rate constant, which can be determined from the PMF following Kramer [81] (see also [82], [83]), and $f^{ii}_{ff}(V)$ its voltage-dependent change. Scheme II needs to be enhanced, however, because the diffusional entry step (Scheme I) constitutes a significant barrier to ion movement through gA channels [84]. Diffusion limitation (DL) becomes important because incoming ions must "hit" the pore entrance rather precisely—meaning that the channel is "hidden" behind a diffusion resistance, which will complicate the mechanistic interpretation of structure-function studies. Furthermore, a potential difference applied across the bilayer (and channel) will change the interfacial ion concentrations; this interfacial polarization (IP) will in its own right have an impact on ion movement through the channel [85]. When the 3B2S2I kinetic model is enhanced to incorporate both DL and interfacial limitation, the resulting 3B2S2I(DL,IP) model provides an acceptable, discrete-state, kinetic description of ion permeation through gA channels (Section III-B).

B. Ion Permeation Through gA Channels

The amino acid side chains do not contact the permeating ions, but the gA channels' permeability properties are modulated by amino acid substitutions throughout the sequence [66], [86]–[90]: nonpolar→polar substitutions in the formyl–NH–terminal half of the sequence tend to reduce the conductance; polar→nonpolar substations in the carboxy-ethanolamide half tend to reduce the conductance. The primary mechanism by which amino acid substitutions alter the ion permeability appears to be electrostatic interactions between the permeating ions and the side chain dipoles [66], [90], [91].

The kinetics of ion movement through gA channels have been studied using single-channel measurements in glycerol-monoleate [74], [92]–[94] or DPhPC [95] bilayers. Figs. 8 and 9 show results obtained in DPhPC/*n*-decane with Na^+ as

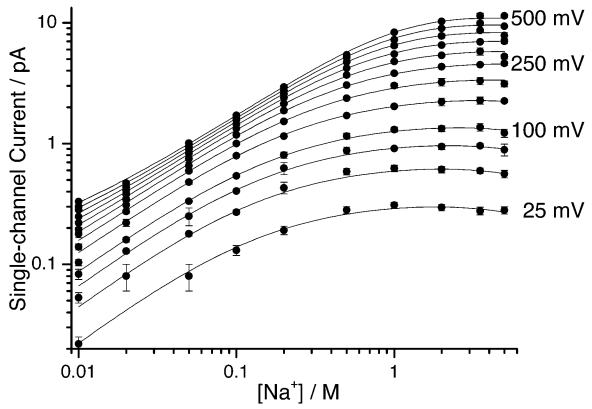

Fig. 8. Current–voltage–concentration (*i-V-C*) results for Na^+ moving through gA channels in DPhPC bilayers and fit of the 3B2S2I(DL,IP) model to the results. 25 °C. (O. S. Andersen and M. D. Becker, unpublished observations).

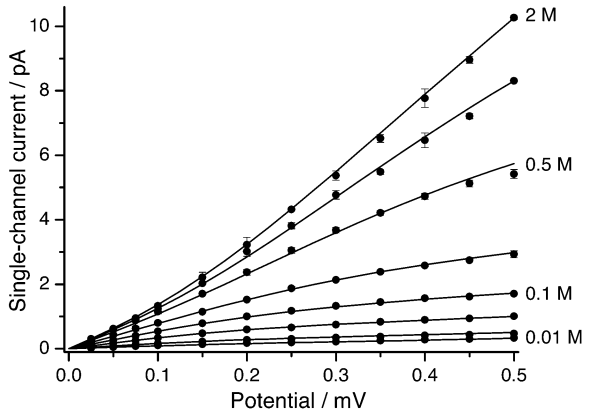

Fig. 9. Current-voltage (*i-V*) results for $[Na^+]$ between 0.01 and 2.0 M and fits of the 3B2S2I(DL,IP) model to the results. Results from Fig. 8.

the permeant ion, as well as the fit of the 3B2S2I(DL,IP) model to the results.

The data span a large range of voltages and concentrations. One needs such a large data set to evaluate discrete-state kinetic models—as well as more detailed, physical descriptions of ion movement through a channel—because the *i-V* relations are fairly linear. That is, the individual data points are highly correlated, such that the information content per point is limited. It is particularly important to have results at high potentials (at both low permeant ion concentrations, where the ion entry step is rate limiting, and high permeant concentrations, where ion exit becomes limiting).

At $[Na^+] \leq 0.1$ M, or so, the *i-V* relations tend to level off toward a voltage-independent limit as *V* increases [84] because the rate of ion movement becomes determined by the voltage-independent diffusion step (Scheme I). (The unavoidable IP causes the interfacial cation to increase at the positive channel entrance [85], and a *bona fide* voltage-dependent limit is attained only in the limit where the ionic strength (due to inert salt, which does not permeate or block the channels) is much higher than the permeant cation concentration [85].) This limiting current allows for the determination of the diffusion-limited ion access rate constant κ_0 ($\approx 2 \cdot \pi \cdot r_0$, where r_0 is the channel's capture radius for the ion, the difference between the effective pore and ion

TABLE I
KINETICS OF Na^+ PERMEATION THROUGH gA CHANNELS AND Trp→Phe SUBSTITUTED gA CHANNELS

Trp→Phe substitution Rate Constant	None	Position 9	Position 15
κ_0 / $M^{-1}\cdot s^{-1}\cdot 10^7$	9	9	9
κ_{I0}^{00} / $M^{-1}\cdot s^{-1}\cdot 10^7$	41	51	7
κ_{00}^{I0} / $s^{-1}\cdot 10^7$	11	26	4.6
κ_{0I}^{I0} / $s^{-1}\cdot 10^6$	7	2.3	4.7
κ_{II}^{0I} / $M^{-1}\cdot s^{-1}\cdot 10^7$	0.7	0.02	0.005
κ_{0I}^{II} / $s^{-1}\times 10^7$	2.8	0.3	0.02

The rate constants, apart from κ_0, are defined in Scheme II and (5). The SDs, determined from Monte Carlo-based error analysis, usually are less than 10%; always less than 20%. From Becker *et al.* [95].

TABLE II
DERIVED PARAMETERS FOR Na^+ PERMEATION THROUGH gA CHANNELS AND Trp→Phe SUBSTITUTED gA CHANNELS

Trp→Phe substitution Parameter	None	Position 9	Position 15
K_I / M	0.14	0.25	0.32
K_{II} / M	8	38	13
K_I/K_{II}	58	150	39
κ_{II}^{0I} / κ_{I0}^{00}	0.02	0.004	0.007
κ_{0I}^{II} / κ_{00}^{I0}	0.25	0.01	0.007

The entries are calculated based on the parameters in Table I, based on an Monte Carlo-based error analysis.

radii), which is $\sim 10^8\ M^{-1}\cdot s^{-1}$ for Na^+ and $\sim 2\cdot 10^8\ M^{-1}\cdot s^{-1}$ for the higher alkali metal cations [84].

Assuming that the ion's diffusion coefficient close to the pore entrance is equal to the bulk diffusion coefficient, which is questionable [96], the channel's capture radius for the alkali metal cations is ~ 0.3 Å. This provides for an estimate of the ions' thermal velocity (v_0), because the ions' overall collision rate with the pore entrance is $v_0\cdot 2\cdot\pi\cdot r_0^2\cdot C_0$, where C_0 is the ion concentration at the pore entrance, whereas the diffusion-limited rate of ion-channel encounters is $2\cdot\pi\cdot r_0\cdot D\cdot(C_b-C_0)$, where C_b is the bulk ion concentration. When $r_0 > 1$ Å, as for diffusion-limited reactions in bulk solutions, the diffusion-limited step is rate limiting. When $r_0 < 1$ Å, the relative resistance imposed by the collision step becomes increasingly important as r_0 decreases, which makes it possible to estimate v_0 to be $\sim 10^4$ cm/s [97], as predicted by Einstein [98].

At $[Na^+] > 1$ M, when the channel usually is occupied by an ion, the slope of *i-V* relations increases as *V* increases (Fig. 9) because the rate of ion movement becomes determined by voltage-dependent transitions within the pore (translocation and exit, Scheme I). That is, by examining the *i-V-C* relations over a large range of ion concentrations and applied potentials, it is possible to explore the various steps in the ion movement through the pore—and to determine the underlying rate constants. Table I summarizes results obtained with gA, as well as two Trp→Phe-substituted gA analogues [Phe^9]gA and [Phe^{15}]gA that form channels, structurally equivalent to gA channels, with conductances (in 1.0 M NaCl at 200-mV applied potential) of 6.0 and 10.9 pS, respectively, as compared to 15.0 pS for gA channels [67].

The predicted Na^+ affinities (defined by $K_I = \kappa_{00}^{I0}/(2\cdot\kappa_{I0}^{00})$ and K_{II} $(= 2\cdot\kappa_{0I}^{II}/\kappa_{II}^{0I})$, where the factors of two arise because ions can enter from either side of an empty pore and leave from either side of a doubly occupied pore), are listed in Table II. To appreciate the channels' affinity for Na^+, it is useful to compare the Na^+ mole-fraction (n_{Na}) in the pore (n_{Na}^{pore}), with $\sim 6H_2O$ molecules in the single-filing stretch [72], [73] to n_{Na} in the bulk solution (n_{Na}^{bulk}). At 0.14 M, $n_{Na}^{bulk} \approx 1/400$, whereas $n_{Na}^{pore} \approx 0.1$ (corresponding to a 5-M solution) or ∼40-fold higher than in the bulk solution. Na^+, therefore, is preferentially solvated by the pore lining, as compared with the bulk H_2O. A similar conclusion can be drawn for other ion-conducting channels [29].

It is now possible to estimate the channels' catalytic rate enhancement, the rate of channel-catalyzed ion movement relative to noncatalyzed movement through the bilayer k_{cat}/k_{non} [99]. To a first approximation, $k_{cat}/k_{non} = K_{p/w}/K_{m/w}$, where $K_{p/w}$ and $K_{m/w}$ denote the ion partition coefficients into the pore and into the bilayer hydrophobic core, respectively, in the limit where the ion occupancy is $\ll 1$. $K_{p/w} \approx n_{Na}^{pore}/n_{Na}^{bulk} \approx 10^2$; $K_{m/w}$ can be estimated to be $\sim 10^{-14}$ based on the conductance (G_0) of unmodified bilayers in 1.0 M NaCl, $\sim 10^{-9}$ S/cm^2 [100] using the relation [101], [102]

$$G_0 = N_A\cdot\frac{(ze)^2}{k_BT}\cdot\frac{D_m}{d_0}\cdot K_{\frac{m}{w}}\cdot C. \tag{6}$$

We, thus, find that the catalytic rate enhancement is $\sim 10^{16}$, which is comparable to conventional enzymes [99].

C. Ion–Ion Interactions May Be Water-Mediated

Tables I and II show that $K_{II}/K_I \gg 1$, indicative of repulsive ion–ion interactions; but the ratio differs among the channels, suggesting that ion–ion interactions within the doubly occupied channels are not due solely to electrostatic interactions. This conclusion is supported by examining the ratios of association and dissociation rate constants for the first and the second ion entering (or leaving), the lower two lines in Table II. Both ratios are decreased—with the major decrease being in the association rate constant ratio. This surprising result presumably means that the water in the pore (being relatively incompressible) plays an important role in mediating ion–ion interactions; see also [103]. It further suggests that the pore water needs to be considered in Brownian dynamics (BD) simulations of channel-catalyzed ion movement.

D. Importance of the Trp Residues for Ion Permeation

The four Trp residues at the pore entrance are important for both channel folding and channel function. They are oriented with their dipole moments directed away from the channel center (the NHs toward the aqueous solution [31], [32], [34], which will lower the central electrostatic barrier below that

estimated using a structure-less dielectric model [91], [104], [105].

Consistent with this idea, gA analogues with one or more Trp→Phe replacements form channels with decreased ion permeabilities [67]; see Section III-B. When all four Trp residues are replaced by Phe, the Cs^+ conductance is reduced sixfold [68]. The basis for the reduced conductance appears to be a greatly reduced rate constant for ion translocation through the channel, κ_{0I}^{f0} [106], although ion entry is also altered [68]. The latter could arise because the amphipathic indoles may be able to move (a little) out beyond the hydrophobic membrane core, which could be important as an incoming ion sheds most of its hydration shell to become solvated by the peptide backbone. The backbone deformation that is needed to optimize ion–oxygen contacts [107] will involve also side chain motions [108].

The changes in Na^+ permeation through single Trp→Phe substituted gramicidins has been examined in detail [95]; see Tables I and II. The kinetic analysis provides information about rate constants for ion translocation, but no information about the absolute barrier heights (and well depths) of the free energy profile for ion movement through the pore [82]. Such information can be extracted only through an appropriate physical theory, such as a hierarchical implementation of MD and BD simulations [83]. Nevertheless, it is possible to estimate the *changes* in barrier heights and well depths as $k_BT \cdot \ln\{\kappa^{\text{Analogue}}/\kappa^{\text{Control}}\}$ for each of the transitions along the reaction coordinate [82]. We conclude that single Trp→Phe substitutions at the channel pore entrances (one in each subunit) may alter the barrier profile (decrease well depths, increase barrier heights) by several k_BT.

Trp→Phe substitutions increase in the height of the central barrier. Because the sequence substitutions to do not alter the structure of the subunit interface [67], the conductance changes most likely result from favorable electrostatic interactions between the indole dipole and the permeant ion [91]. Surprisingly, the sign of the Trp→Phe substitution-induced changes in the entry/exit barrier depends on the position where the substitution is made, indicating that the side chain dynamics indeed are important for the rate of the ions' hydration/solvation.

IV. Molecular Dynamics Analysis of Ion Permeation

To obtain better insights into the molecular basis for channel (or membrane protein) function, it is necessary to establish direct links between the atomic structure of a channel (or protein) and its observed function. Though MD simulations, in principle, should provide the desired tool [109], one cannot reach the necessary level of insight through "brute force" MD simulations [83], [110], because the ion flux typically corresponds to a net flux of one ion in ∼100 ns—much longer than typical MD trajectories [110]. Indeed, when using MD simulations to predict the PMF for ion movement through gA channels, the barrier heights are too high by many kcal/mol [111]. This is of concern because the small and relatively well-behaved gA channels should be particularly amenable to in-depth theoretical analysis and computer simulations.

There is reason for optimism, nevertheless. Fig. 10 shows two PMFs (free energy profiles) for K^+ permeation through

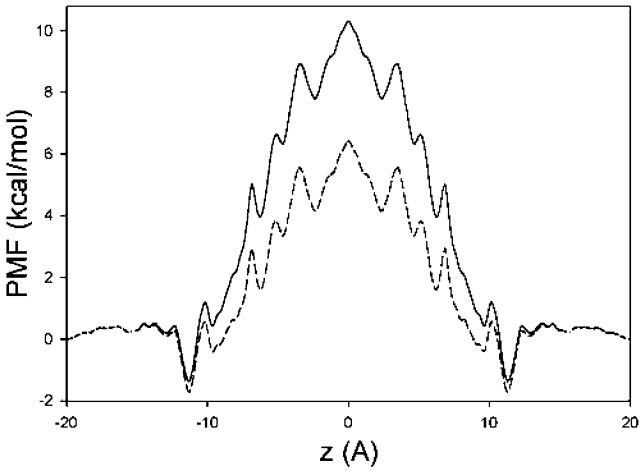

Fig. 10. One-dimensional (1-D) PMF, or free energy profile, for K^+ along the gA axis. The upper solid curve denotes the initial result of MD simulations. The free energy profile is not meaningful beyond the cuts at $z = 15$ Å because no absolute reference of such a 1-D PM can be defined for large z [83]. The lower dashed curve denotes the PMF corrected for size, and membrane dielectric constant (see text). From Allen *et al.* [112].

gA channels. The main structural features of the PMFs, i.e., two cation binding sites near the channel's end separated by a central barrier, are both qualitatively consistent with Scheme I, which has been deduced from experiments [78], [79]. From a quantitative point of view, however, the "uncorrected" PMF (——) displays a central barrier that is markedly too high, a problem similar to what has been observed in previous studies and which must be addressed. After correcting for two potentially serious artifacts, however, the resulting PMF (– – –) predicts results that are in semiquantitative agreement with experimental results. The first artifact is introduced by the periodic boundary conditions of the finite simulation system, which cause a spurious destabilization of the permeating ion in the channel relative to the bulk (this disappears if the system becomes exceedingly large) [113]. The second artifact arises because the hydrocarbon chains of the lipids are not polarizable in MD force fields, such that this region is treated as corresponding to a dielectric constant of one, whereas it should be two [114], the dielectric constant of bulk hydrocarbons, or even higher [115].

It is possible to correct for these artifactual contributions by a continuum electrostatic approximation using the configurations of the MD trajectories to average over protein and single-file water configurations. This analysis shows that the periodic boundary conditions cause a spurious repulsion on the order of 2 kcal/mole when the ion is in the middle of the channel and that a change of dielectric constant for the bilayer core from one to two stabilizes the ion in the channel by about 2 kcal/mole. The barrier in the corrected PMF, therefore, is about 4 kcal/mole lower than in the original PMF, which corresponds to a thousandfold change in the predicted ion permeability. Indeed, the maximal conductance for K^+ is predicted to be 0.8 pS, "only" 30-fold less than the measured value (in 1.0 M KCl).

Some problems persist because the location and depth of the predicted binding sites differ somewhat from the experimental values [78], [79]: the binding sites are too far from the channel center and too shallow to be compatible with the observed ion

affinities; but the predicted affinity ($K_I \approx 0.34$ M) differs only by a factor of five from the one predicted from the kinetic analysis of *i-V-C* results in gA channels ($K_I \approx 0.07$ M; O. S. Andersen and M. D. Becker, unpublished results). Both problems are likely to result from the use of nonpolarizable force fields to evaluate the ion-peptide interactions, which, therefore, will tend to be underestimated. Because the PMF effectively arises as the sum of contributions from the permeating ion's interaction with the channel peptide, the single-filing water in the pore, and the bilayer hydrophobic core [112], both the position and depth of the energy minima will be particularly sensitive to the choice of force fields.

Given the progress that is taking place in terms of developing force fields that include induced polarization [116]–[118], there is every reason to be optimistic about the future. Indeed, even the present generation of force fields predicts changes in the central barrier (which should reflect primarily long-range electrostatic interactions) that are in near-quantitative agreement with experimental results (T. W. Allen, O. S. Andersen and B. Roux, unpublished results), which suggests that one with some confidence can begin to use MD to understand the basis for amino acid substitution-induced *changes* in channel function.

V. Conclusion

The well-defined functional and structural features of gramicidin channels provide detailed insights into the molecular basis for channel function. The modest channel size further allows for detailed computational analysis, which promises to provide atomic-level insights into the microphysics underlying ion permeation. This combination of features remains unprecedented and suggests that the gA channels will become increasingly important as test beds for theoretical models of channel-catalyzed ion permeation.

Acknowledgment

The authors would like to thank T. W. Allen, M. D. Becker, A. E. Daily, D. V. Greathouse, S. Shobana, and S. E. Tape for stimulating discussions and technical assistance.

References

[1] F. M. Harold and J. R. Baarda, "Gramicidin, valinomycin, and cation permeability of *Streptococcus faecalis*," *J. Bacteriol.*, vol. 94, pp. 53–60, 1967.

[2] S. B. Hladky and D. A. Haydon, "Discreteness of conductance change in bimolecular lipid membranes in the presence of certain antibiotics," *Nature*, vol. 225, pp. 451–453, 1970.

[3] D. W. Urry, "The gramicidin A transmembrane channel: a proposed $\pi_{(L,D)}$ helix," *Proc. Nat. Acad. Sci. USA*, vol. 68, pp. 672–676, 1971.

[4] ——, "Protein conformation in biomembranes: optical rotation and absorption of membrane suspensions," *Biochim. Biophys. Acta*, vol. 265, pp. 115–168, 1972.

[5] M. S. Weiss, A. Kreusch, E. Schiltz, U. Nestel, W. Welte, J. Weckesser, and G. E. Schulz, "The structure of porin from *Rhodobacter capsulatus* at 1.8 Å resolution," *FEBS Lett.*, vol. 280, pp. 379–382, 1991.

[6] S. W. Cowan *et al.*, "Crystal structures explain functional properties of two E. coli porins," *Nature*, vol. 358, pp. 727–733, 1992.

[7] D. A. Doyle *et al.*, "The structure of the potassium channel: molecular basis of K^+ conduction and selectivity," *Science*, vol. 280, pp. 69–77, 1998.

[8] G. Chang, R. H. Spencer, A. T. Lee, M. T. Barclay, and D. C. Rees, "Structure of the MscL homolog from *Mycobacterium tuberculosis*: a gated mechanosensitive ion channel," *Science*, vol. 282, pp. 2220–2226, 1998.

[9] R. B. Bass, P. Strop, M. Barclay, and D. C. Rees, "Crystal structure of *Escherichia coli* MscS, a voltage-modulated and mechanosensitive channel," *Science*, vol. 298, pp. 1582–1587, 2002.

[10] Y. Jiang, A. Lee, J. Chen, M. Cadene, B. T. Chait, and R. MacKinnon, "The open pore conformation of potassium channels," *Nature*, vol. 417, pp. 523–526, 2002.

[11] Y. Jiang, A. Lee, J. Chen, V. Ruta, M. Cadene, B. T. Chait, and R. MacKinnon, "X-ray structure of a voltage-dependent K^+ channel," *Nature*, vol. 423, pp. 33–41, 2003.

[12] A. Kuo *et al.*, "Crystal structure of the potassium channel KirBac1.1 in the closed state," *Science*, vol. 300, pp. 1922–1926, 2003.

[13] A. Miyazawa, Y. Fujiyoshi, and N. Unwin, "Structure and gating mechanism of the acetylcholine receptor pore," *Nature*, vol. 423, pp. 949–955, 2003.

[14] R. Sarges and B. Witkop, "Gramicidin A. V. The structure of valine- and isoleucine-gramicidin A," *J. Amer. Chem. Soc.*, vol. 87, pp. 2011–2019, 1965.

[15] G. N. Ramachandran and R. Chandrasekaran, "Studies on dipeptide conformation and on peptides with sequences of alternating L and D residues with special reference to antibiotic and ion transport peptides," *Prog. Peptides Res.*, vol. 2, pp. 195–215, 1972.

[16] W. R. Veatch, E. T. Fossel, and E. R. Blout, "The conformation of gramicidin A," *Biochemistry*, vol. 13, pp. 5249–5256, 1974.

[17] W. R. Veatch and E. R. Blout, "The aggregation of gramicidin A in solution," *Biochemistry*, vol. 13, pp. 5257–5264, 1974.

[18] V. F. Bystrov and A. S. Arseniev, "Diversity of the gramicidin A spatial structure: two-dimensional proton NMR study in solution," *Tetrahedron*, vol. 44, pp. 925–940, 1988.

[19] D. A. Langs, "Three-dimensional structure at 0.86 Å of the uncomplexed form of the transmembrane ion channel peptide gramicidin A," *Science*, vol. 241, pp. 188–191, 1988.

[20] B. M. Burkhart, N. Li, D. A. Langs, W. A. Pangborn, and W. L. Duax, "The conducting form of gramicidin A is a right-handed double-stranded double helix," *Proc. Nat. Acad. Sci. USA*, vol. 95, pp. 12 950–12 955, 1998.

[21] N. Abdul-Manan and J. F. Hinton, "Conformational states of gramicidin A along the pathway to the formation of channels in model membranes determined by 2D NMR and circular dichroism spectroscopy," *Biochemistry*, vol. 33, pp. 6773–6783, 1994.

[22] S. B. Hladky and D. A. Haydon, "Ion transfer across lipid membranes in the presence of gramicidin A. I. Studies of the unit conductance channel," *Biochim. Biophys. Acta*, vol. 274, pp. 294–312, 1972.

[23] V. B. Myers and D. A. Haydon, "Ion transfer across lipid membranes in the presence of gramicidin A. II. Ion selectivity," *Biochim. Biophys. Acta*, vol. 274, pp. 313–322, 1972.

[24] A. Finkelstein, "Aqueous pores created in thin lipid membranes by the antibiotics nystatin, amphotericin B and gramicidin A. Implications for pores in plasma membranes," in *Drugs and Transport Processes*, B. A. Callingham, Ed. London, U.K.: MacMillan, 1974, pp. 241–250.

[25] E. Bamberg, H. J. Apell, and H. Alpes, "Structure of the gramicidin A channel: discrimination between the $\pi_{L,D}$ and the β helix by electrical measurements with lipid bilayer membranes," *Proc. Nat. Acad. Sci. USA*, vol. 74, pp. 2402–2406, 1977.

[26] W. Veatch and L. Stryer, "The dimeric nature of the gramicidin A transmembrane channel: conductance and fluorescence energy transfer studies of hybrid channels," *J. Mol. Biol.*, vol. 113, pp. 89–102, 1977.

[27] S. Weinstein, B. A. Wallace, E. R. Blout, J. S. Morrow, and W. Veatch, "Conformation of gramicidin A channel in phospholipid vesicles: a carbon-13 and fluorine-19 nuclear magnetic resonance study," *Proc. Nat. Acad. Sci. USA*, vol. 76, pp. 4230–4234, 1979.

[28] S. Weinstein, B. A. Wallace, J. S. Morrow, and W. R. Veatch, "Conformation of the gramicidin A transmembrane channel: a 13C nuclear magnetic resonance study of 13C-enriched gramicidin in phosphatidylcholine vesicles," *J. Mol. Biol.*, vol. 143, pp. 1–19, 1980.

[29] O. S. Andersen and R. E. Koeppe II, "Molecular determinants of channel function," *Physiol. Rev.*, vol. 72, pp. S89–S158, 1992.

[30] A. S. Arseniev, I. L. Barsukov, V. F. Bystrov, and Y. A. Ovchinnikov, "Spatial structure of a gramicidin A transmembrane ion channel. NMR analysis in micelles," *Biol. Membr.*, vol. 3, pp. 437–462, 1986.

[31] R. R. Ketchem, B. Roux, and T. A. Cross, "High-resolution polypeptide structure in a lamellar phase lipid environment from solid state NMR derived orientational constraints," *Structure*, vol. 5, pp. 1655–1669, 1997.

[32] L. E. Townsley, W. A. Tucker, S. Sham, and J. F. Hinton, "Structures of gramicidins A, B, and C incorporated into sodium dodecyl sulfate micelles," *Biochemistry*, vol. 40, pp. 11 676–11 686, 2001.

[33] T. W. Allen, O. S. Andersen, and B. Roux, "The structure of gramicidin A in a lipid bilayer environment determined using molecular dynamics simulations and solid-state NMR data," *J. Amer. Chem. Soc.*, vol. 125, pp. 9868–9878, 2003.

[34] A. S. Arseniev, A. L. Lomize, I. L. Barsukov, and V. F. Bystrov, "Gramicidin A transmembrane ion-channel. Three-dimensional structure reconstruction based on NMR spectroscopy and energy refinement," *Biol. Membr.*, vol. 3, pp. 1077–1104, 1986.

[35] R. R. Ketchem, W. Hu, and T. A. Cross, "High-resolution conformation of gramicidin A in a lipid bilayer by solid-state NMR," *Science*, vol. 261, pp. 1457–1460, 1993.

[36] C. M. Nimigean and C. Miller, "Na^+ block and permeation in a K^+ channel of known structure," *J. Gen. Physiol.*, vol. 120, p. 323, Aug 26, 2002.

[37] J. B. Park, H. J. Kim, P. D. Ryu, and E. Moczydlowski, "Effect of phosphatidylserine on unitary conductance and Ba^{2+} block of the BK Ca^{2+}-activated K^+ channel: re-examination of the surface charge hypothesis," *J. Gen. Physiol.*, vol. 121, pp. 375–398, 2003.

[38] A. M. O'Connell, R. E. Koeppe II, and O. S. Andersen, "Kinetics of gramicidin channel formation in lipid bilayers: transmembrane monomer association," *Science*, vol. 250, pp. 1256–1259, 1990.

[39] J. T. Durkin, L. L. Providence, R. E. Koeppe II, and O. S. Andersen, "Formation of non-β-helical gramicidin channels between sequence-substituted gramicidin analogues," *Biophys. J.*, vol. 62, pp. 145–159, 1992.

[40] O. S. Andersen *et al.*, "Gramicidin channel controversy—The structure in a lipid environment," *Nature Struct. Biol.*, vol. 6, p. 609, 1999.

[41] D. Salom, M. C. Bańo, L. Braco, and C. Abad, "HPLC demonstration that an all Trp→Phe replacement in gramicidin A results in a conformational rearrangement from beta-helical monomer to double-stranded dimer in model membranes," *Biochem. Biophys. Res. Commun.*, vol. 209, pp. 466–473, 1995.

[42] D. Salom, E. Perez-Paya, J. Pascal, and C. Abad, "Environment- and sequence-dependent modulation of the double-stranded to single-stranded conformational transition of gramicidin A in membranes," *Biochemistry*, vol. 37, pp. 14 279–14 291, 1998.

[43] J. A. Killian and G. von Heijne, "How proteins adapt to a membrane-water interface," *Trends Biochem. Sci.*, vol. 25, pp. 429–434, 2000.

[44] B. A. Cornell, F. Separovic, A. J. Baldassi, and R. Smith, "Conformation and orientation of gramicidin A in oriented phospholipid bilayers measured by solid state carbon-13 NMR," *Biophys. J.*, vol. 53, pp. 67–76, 1988.

[45] L. K. Nicholson, F. Moll, T. E. Mixon, P. V. LoGrasso, J. C. Lay, and T. A. Cross, "Solid-state 15N NMR of oriented lipid bilayer bound gramicidin A′," *Biochemistry*, vol. 26, pp. 6621–6626, 1987.

[46] J. A. Killian, M. J. Taylor, and R. E. Koeppe II, "Orientation of the valine-1 side chain of the gramicidin transmembrane channel and implications for channel functioning. A^2 H NMR study," *Biochemistry*, vol. 31, pp. 11 283–11 290, 1992.

[47] F. Separovic, R. Pax, and B. Cornell, "NMR order parameter analysis of a peptide plane aligned in a lyotropic liquid crysta," *Mol. Phys.*, vol. 78, pp. 357–369, 1993.

[48] R. E. Koeppe II, H. Sun, P. C. van der Wel, E. M. Scherer, P. Pulay, and D. V. Greathouse, "Combined experimental/theoretical refinement of indole ring geometry using deuterium magnetic resonance and ab initio calculations," *J. Amer. Chem. Soc.*, vol. 125, pp. 12 268–12 276, 2003.

[49] K. C. Lee, S. Huo, and T. A. Cross, "Lipid-peptide interface: valine conformation and dynamics in the gramicidin channel," *Biochemistry*, vol. 34, pp. 857–867, 1995.

[50] R. E. Koeppe II, J. A. Killian, and D. V. Greathouse, "Orientations of the tryptophan 9 and 11 side chains of the gramicidin channel based on deuterium nuclear magnetic resonance spectroscopy," *Biophys. J.*, vol. 66, pp. 14–24, 1994.

[51] S. F. Scarlata, "The effects of viscosity on gramicidin tryptophan rotational motion," *Biophys. J.*, vol. 54, pp. 1149–1157, 1988.

[52] S. Mukherjee and A. Chattopadhyay, "Motionally restricted tryptophan environments at the peptide-lipid interface of gramicidin channels," *Biochemistry*, vol. 33, pp. 5089–5097, 1994.

[53] D. V. Greathouse, J. F. Hinton, K. S. Kim, and R. E. Koeppe II, "Gramicidin A/short-chain phospholipid dispersions: chain length dependence of gramicidin conformation and lipid organization," *Biochemistry*, vol. 33, pp. 4291–4299, 1994.

[54] O. G. Mouritsen and M. Bloom, "Mattress model of lipid-protein interactions in membranes," *Biophys. J.*, vol. 46, pp. 141–153, 1984.

[55] N. Mobashery, C. Nielsen, and O. S. Andersen, "The conformational preference of gramicidin channels is a function of lipid bilayer thickness," *FEBS Lett.*, vol. 412, pp. 15–20, 1997.

[56] T. P. Galbraith and B. A. Wallace, "Phospholipid chain length alters the equilibrium between pore and channel forms of gramicidin," *Faraday Discuss.*, pp. 159–164, 1998.

[57] H. W. Huang, "Deformation free energy of bilayer membrane and its effect on gramicidin channel lifetime," *Biophys. J.*, vol. 50, pp. 1061–1070, 1986.

[58] J. A. Lundbæk and O. S. Andersen, "Spring constants for channel-induced lipid bilayer deformations—estimates using gramicidin channels," *Biophys. J.*, vol. 76, pp. 889–895, 1999.

[59] M. C. Wiener and S. H. White, "Structure of a fluid dioleoylphosphatidylcholine bilayer determined by joint refinement of X-ray and neutron diffraction data. III. Complete structure," *Biophys. J.*, vol. 61, pp. 437–447, 1992.

[60] E. Lindahl and O. Edholm, "Mesoscopic undulations and thickness fluctuations in lipid bilayers from molecular dynamics simulations," *Biophys. J.*, vol. 79, p. 426, 2000.

[61] C. Nielsen, M. Goulian, and O. S. Andersen, "Energetics of inclusion-induced bilayer deformations," *Biophys. J.*, vol. 74, pp. 1966–1983, 1998.

[62] J. R. Elliott, D. Needham, J. P. Dilger, and D. A. Haydon, "The effects of bilayer thickness and tension on gramicidin single-channel lifetime," *Biochim. Biophys. Acta*, vol. 735, pp. 95–103, 1983.

[63] B. A. Cornell, F. Separovic, D. E. Thomas, A. R. Atkins, and R. Smith, "Effect of acyl chain length on the structure and motion of gramicidin A in lipid bilayers," *Biochim. Biophys. Acta*, vol. 985, pp. 229–232, 1989.

[64] J. T. Durkin, R. E. Koeppe II, and O. S. Andersen, "Energetics of gramicidin hybrid channel formation as a test for structural equivalence. Side-chain substitutions in the native sequence," *J. Mol. Biol.*, vol. 211, pp. 221–234, 1990.

[65] J. T. Durkin, L. L. Providence, R. E. Koeppe II, and O. S. Andersen, "Energetics of heterodimer formation among gramicidin analogues with an NH_2-terminal addition or deletion. Consequences of a missing residue at the join in channel," *J. Mol. Biol.*, vol. 231, pp. 1102–1121, 1993.

[66] J. L. Mazet, O. S. Andersen, and R. E. Koeppe II, "Single-channel studies on linear gramicidins with altered amino acid sequences. A comparison of phenylalanine, tryptophan, and tyrosine substitutions at positions 1 and 11," *Biophys. J.*, vol. 45, pp. 263–276, 1984.

[67] M. D. Becker, D. V. Greathouse, R. E. Koeppe II, and O. S. Andersen, "Amino acid sequence modulation of gramicidin channel function. Effects of tryptophan-to-phenylalanine substitutions on the single-channel conductance and duration," *Biochemistry*, vol. 30, pp. 8830–8839, 1991.

[68] V. Fonseca, P. Daumas, L. Ranjalahy-Rasoloarijao, F. Heitz, R. Lazaro, Y. Trudelle, and O. S. Andersen, "Gramicidin channels that have no tryptophan residues," *Biochemistry*, vol. 31, pp. 5340–5350, 1992.

[69] A. R. Jude, D. V. Greathouse, R. E. Koeppe II, L. L. Providence, and O. S. Andersen, "Modulation of gramicidin channel structure and function by the aliphatic 'spacer' residues 10, 12, and 14 between the tryptophans," *Biochemistry*, vol. 38, pp. 1030–1039, 1999.

[70] G. L. Mattice, R. E. Koeppe II, L. L. Providence, and O. S. Andersen, "Stabilizing effect of D-alanine^2 in gramicidin channels," *Biochemistry*, vol. 34, pp. 6827–6837, 1995.

[71] S. S. Sham *et al.*, "The structure, cation binding, transport, and conductance of Gly_{15}-gramicidin A incorporated into SDS micelles and PC/PG vesicles," *Biochemistry*, vol. 42, pp. 1401–1409, 2003.

[72] D. G. Levitt, S. R. Elias, and J. M. Hautman, "Number of water molecules coupled to the transport of sodium, potassium and hydrogen ions via gramicidin, nonactin or valinomycin," *Biochim. Biophys. Acta*, vol. 512, pp. 436–451, 1978.

[73] P. A. Rosenberg and A. Finkelstein, "Interaction of ions and water in gramicidin A channels: streaming potentials across lipid bilayer membranes," *J. Gen. Physiol.*, vol. 72, pp. 327–340, 1978.

[74] E. Neher, J. Sandblom, and G. Eisenman, "Ionic selectivity, saturation, and block in gramicidin A channels. II. Saturation behavior of single channel conductances and evidence for the existence of multiple binding sites in the channel," *J. Membr. Biol.*, vol. 40, pp. 97–116, 1978.

[75] O. S. Andersen, "Ion movement through gramicidin A channels. Single-channel measurements at very high potentials," *Biophys. J.*, vol. 41, pp. 119–133, 1983.

[76] B. A. Wallace, W. R. Veatch, and E. R. Blout, "Conformation of gramicidin A in phospholipid vesicles: circular dichroism studies of effects of ion binding, chemical modification, and lipid structure," *Biochemistry*, vol. 20, pp. 5754–5760, 1981.

[77] F. Tian and T. A. Cross, "Cation transport: an example of structural based selectivity," *J. Mol. Biol.*, vol. 285, pp. 1993–2003, 1999.

[78] D. W. Urry, T. L. Trapane, C. M. Venkatachalam, and R. B. McMichens, "Ion interactions at membranous polypeptide sites using nuclear magnetic resonance: determining rate and binding constants and site locations," *Methods Enzymol.*, vol. 171, pp. 286–342, 1989.
[79] G. A. Olah, H. W. Huang, W. Liu, and Y. Wu, "Location of ion-binding sites in the gramicidin channel by X-ray diffraction," *J. Mol. Biol.*, vol. 218, pp. 847–858, 1991.
[80] L. V. Schagina, A. E. Grinfeldt, and A. A. Lev, "Interaction of cation fluxes in gramicidin A channels in lipid bilayer membranes," *Nature*, vol. 273, pp. 243–245, 1978.
[81] H. A. Kramers, "Brownian motion in a field of force and the diffusion model of chemical reactions," *Physica*, vol. 7, pp. 284–304, 1940.
[82] O. S. Andersen, "Kinetics of ion movement mediated by carriers and channels," *Methods Enzymol.*, vol. 171, pp. 62–112, 1989.
[83] B. Roux, T. W. Allen, T. W. Bernèche, and W. Im, "Theoretical and computational models of biological ion channels," *Q. Rev. Biophys.*, vol. 37, pp. 15–103, 2004.
[84] O. S. Andersen, "Ion movement through gramicidin A channels. Studies on the diffusion-controlled association step," *Biophys. J.*, vol. 41, pp. 147–165, 1983.
[85] ——, "Ion movement through gramicidin A channels. Interfacial polarization effects on single-channel current measurements," *Biophys. J.*, vol. 41, pp. 135–146, 1983.
[86] E. Bamberg, K. Noda, E. Gross, and P. Läuger, "Single-channel parameters of gramicidin A, B, and C," *Biochim. Biophys. Acta*, vol. 419, pp. 223–228, 1976.
[87] J. S. Morrow, W. R. Veatch, and L. Stryer, "Transmembrane channel activity of gramicidin A analogs: effects of modification and deletion of the amino-terminal residue," *J. Mol. Biol.*, vol. 132, pp. 733–738, 1979.
[88] F. Heitz, G. Spach, and Y. Trudelle, "Single channels of 9,11,13,15-destryptophyl-phenylalanyl-gramicidin A," *Biophys. J.*, vol. 40, pp. 87–89, 1982.
[89] E. W. B. Russell, L. B. Weiss, F. I. Navetta, R. E. Koeppe II, and O. S. Andersen, "Single-channel studies on linear gramicidins with altered amino acid side chains. Effects of altering the polarity of the side chain at position 1 in gramicidin A," *Biophys. J.*, vol. 49, pp. 673–686, 1986.
[90] R. E. Koeppe II, J.-L. Mazet, and O. S. Andersen, "Distinction between dipolar and inductive effects in modulating the conductance of gramicidin channels," *Biochemistry*, vol. 29, pp. 512–520, 1990.
[91] O. S. Andersen, D. V. Greathouse, L. L. Providence, M. D. Becker, and R. E. Koeppe II, "Importance of tryptophan dipoles for protein function: 5-fluorination of tryptophans in gramicidin A channels," *J. Amer. Chem. Soc.*, vol. 120, pp. 5142–5146, 1998.
[92] C. D. Cole, A. S. Frost, N. Thompson, M. Cotten, T. A. Cross, and D. D. Busath, "Noncontact dipole effects on channel permeation. VI. 5F-and 6F-Trp gramicidin channel currents," *Biophys. J.*, vol. 83, pp. 1974–1986, 2002.
[93] B. W. Urban, S. B. Hladky, and D. A. Haydon, "Ion movements in gramicidin pores. An example of single-file transport," *Biochim. Biophys. Acta*, vol. 602, pp. 331–354, 1980.
[94] D. D. Busath *et al.*, "Noncontact dipole effects on channel permeation. I. Experiments with (5F-indole) Trp^{13} gramicidin A channels," *Biophys. J.*, vol. 75, pp. 2830–2844, 1998.
[95] M. D. Becker, R. E. Koeppe II, and O. S. Andersen, "Amino acid substitutions and ion channel function: model-dependent conclusions," *Biophys. J.*, vol. 62, pp. 25–27, 1992.
[96] S. König, E. Sackmann, D. Richter, R. Zorn, C. Carlile, and T. M. Bayerl, "Molecular dynamics of water in oriented DPPC multilayers studied by quasielastic neutron scattering and deuterium-nuclear magnetic resonance relaxation," *J. Chem. Phys.*, vol. 100, pp. 3307–3316, 1994.
[97] O. S. Andersen and S. W. Feldberg, "The heterogeneous collision velocity for hydrated ions in aqueous solutions is $\sim 10^4$ cm/s," *J. Phys. Chem.*, vol. 100, pp. 4622–4629, 1996.
[98] A. Einstein, "Theoretische Betrachtungen über der Brownsche Bewegungen," *Zeit. f. Elektrochemie*, vol. 13, pp. 41–42, 1907.
[99] R. Wolfenden and M. J. Snider, "The depth of chemical time and the power of enzymes as catalysts," *Acc. Chem. Res.*, vol. 12, pp. 938–945, 2001.
[100] T. Hanai, D. A. Haydon, and J. Taylor, "The variation of capacitance and conductance of bimolecular lipid membranes with area," *J. Theor. Biol.*, vol. 9, pp. 433–443, 1965.
[101] A. L. Hodgkin and B. Katz, "The effect of sodium ions on the electrical activity of the giant axon of the squid," *J. Physiol.*, vol. 108, pp. 37–77, 1949.
[102] O. S. Andersen, "Elementary aspects of acid-base permeation and pH regulation," *Ann. New York Acad. Sci.*, vol. 574, pp. 333–353, 1989.
[103] B. Roux, B. Prod'hom, and M. Karplus, "Ion transport in the gramicidin channel: molecular dynamics study of single and double occupancy," *Biophys. J.*, vol. 68, pp. 876–892, 1995.
[104] P. C. Jordan, "The total electrostatic potential in a gramicidin channel," *J. Membr. Biol.*, vol. 78, pp. 91–102, 1984.
[105] M. Sancho and G. Martinez, "Electrostatic modeling of dipole-ion interactions in gramicidin like channels," *Biophys. J.*, vol. 60, pp. 81–88, 1991.
[106] D. Caywood, J. Durrant, P. Morrison, and D. D. Busath, "The Trp potential deduced from gramicidin A/gramicidin M channels," *Biophys. J.*, vol. 86, p. 55a, 2004.
[107] S. Y. Noskov, S. Bernèche, and B. Roux, "Control of ion selectivity in potassium channels by electrostatic and dynamic properties of carbonyl ligands," *Nature*, vol. 431, pp. 830–834, 2004.
[108] D. W. Urry, "Polypeptide conformation and biological function: β-helices ($\pi_{L,D}$-helices) as permselective transmembrane channels," in *Proc. Jerusalem Symp. Quant. Chem. Biochem.*, vol. 5, 1973, pp. 723–736.
[109] S. Edwards, B. Corry, S. Kuyucak, and S.-H. Chung, "Continuum electrostatics fails to describe ion permeation in the gramicidin channel," *Biophys. J.*, vol. 83, p. 1348, 2002.
[110] B. Roux, "Theoretical and computational models of ion channels," *Curr. Opin. Struct. Biol.*, vol. 12, pp. 182–189, 2002.
[111] T. W. Allen, T. Bastug, S. Kuyucak, and S.-H. Chung, "Gramicidin A channel as a test ground for molecular dynamics force fields," *Biophys. J.*, vol. 84, p. 2159, 2003.
[112] T. W. Allen, O. S. Andersen, and B. Roux, "Energetics of ion conduction through the gramicidin channel," *Proc. Nat. Acad. Sci. USA*, vol. 101, pp. 117–122, 2004.
[113] P. H. Hünenberger and J. A. McCammon, "Ewald artifacts in computer simulations of ionic solvation and ion–ion interaction: a continuum electrostatics study," *J. Chem. Phys.*, vol. 110, p. 1856, 1999.
[114] J. Åqvist and A. Warshel, "Energetics of ion permeation through membrane channels. Solvation of Na^+ by gramicidin A," *Biophys. J.*, vol. 56, pp. 171–182, 1989.
[115] A. B. Mamanov, R. D. Coalson, A. Nitzan, and M. G. Kurnikova, "The role of the dielectric barrier in narrow biological channels: a novel composite approach to modeling single-channel currents," *Biophys. J.*, vol. 84, pp. 3646–3661, 2003.
[116] G. Lamoureux and B. Roux, "Modeling induced polarizability with classical Drude oscillators: theory and molecular dynamics simulation algorithm.," *J. Chem. Phys.*, pp. 3025–3039, 2003.
[117] V. M. Anisimov, I. V. Vorobyov, G. Lamoureux, S. Noskov, B. Roux, and A. D. MacKerell Jr., "CHARMM all-atom polarizable force field parameter development for nucleic acids," *Biophys. J.*, vol. 86, p. 415a, 2004.
[118] G. Lamoureux, A. D. MacKerell Jr., and B. Roux, "A simple polarizable water model based on classical Drude oscillators," *J. Chem. Phys.*, pp. 5185–5197, 2003.

Olaf S. Andersen received the M.D. degree from University of Copenhagen, Copenhagen, Denmark in 1971.

After postdoctoral training at University of Copenhagen and Rockefeller University, New York (1971–1973), he joined the faculty in the Department of Physiology and Biophysics at Cornell University Medical College (now Weill Medical College of Cornell University), New York, where he is currently Thomas H. Meikle, Jr., Professor of Medical Education. He is Editor of the *Journal of General Physiology*. His primary research interests involve channel-mediated ion movement across lipid bilayers, the elastic properties of lipid bilayer membranes, and the bilayer-dependent regulation of membrane protein function.

Dr. Andersen is a Foreign Member of the Royal Danish Academy of Sciences and Letters and Recipient of the K. S. Cole Medal from the Biophysical Society (1999).

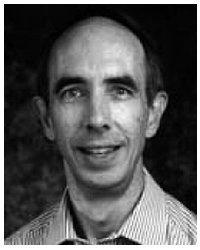

Roger E. Koeppe, II, received the A.B. degree in chemistry from Haverford College, Haverford, PA, in 1971, working with C. MacKay, and the Ph.D. degree in chemistry from the California Institute of Technology, Pasadena, in 1976, working with R. Stroud.

He did postdoctoral work in structural biology with L. Stryer at Stanford University, Stanford, CA, before joining the faculty at the University of Arkansas, Fayetteville, in 1979, where he is currently University Professor of Chemistry and Biochemistry. His primary research interests involve the design and use of model peptides that will shed light on mechanistic details of protein/lipid interactions at the molecular and atomic levels.

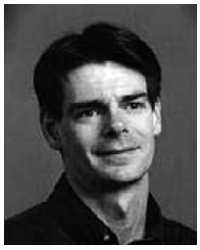

Benoît Roux received the B.S. degree in physics and the M.S. degree in biophysics from the Université de Montréal, Montréal, QC, Canada, in 1981 and 1984, respectively, and the Ph.D. degree in biophysics from Harvard University, Cambridge, MA, in 1990, working under the supervision of M. Karplus.

After a year of postdoctoral research at the Commissariat a l'Energie Atomique, Paris, France he joined the faculty in the Physics and Chemistry Departments at the Université de Montréal. Since 1999, he has been Professor in the Departments of Biochemistry and Physiology and Biophysics at the Weill Medical College, Cornell University, New York. He is one of the developers of the biomolecular simulation program CHARMM. His work has mostly focused on the investigations of the function of ion channels and the development of statistical mechanical methods for computing the solvation-free energy of biological molecules.

In 1998, Dr. Roux was awarded the Rutherford Medal from the Royal Society of Canada and the Noranda Lecture Award from the Chemical Institute of Canada.